Bragg-Cherenkov Scattering and Nonlinear Conductivity of a Two-Dimensional Wigner Crystal

M. I. Dykman and Yuri G. Rubo*
Department of Physics and Astronomy, Michigan State University, East Lansing, Michigan 48824
(Received 11 March 1997)

We show that the conductivity of 2D Wigner crystals displays strong nonlinearity. It arises from coherent many-electron Cherenkov emission of surface waves in the substrate (e.g., ripplons on helium) with the wave vectors $\mathbf{q}$ close to the reciprocal lattice vectors $\mathbf{G}$ of the electron solid. The rate of such Bragg-Cherenkov scattering sharply increases with the Wigner crystal velocity v as $\mathbf{v} \cdot \mathbf{G}$ approaches the surface wave frequency $\omega(G)$. The results are compared with recent experiments. [S0031-9007(97)03468-6]

PACS numbers: 73.20.Dx, 67.90.+z, 73.50.Jt

Recently, several experimental groups [1–3] observed that when electrons above helium surface form a two-dimensional Wigner crystal, they display strongly nonlinear magnetoconductivity, including switching from a high- to a low-conductivity state with increasing driving field. The nonlinearity arises for extremely weak fields where electron heating is negligibly small [3]. The switching was interpreted [2] as being due to the electron crystal sliding out of a periodic array of polaron-type "dimples" on the helium surface [4]. However, the strong nonlinearity of the conductivity, which is observed even well below the switching [3], has remained unexplained. In the present paper we show that such nonlinearity is a generic feature of the transport of electron solids. It is due to the mechanism of electron *losses* which we call the Bragg-Cherenkov scattering. This mechanism describes basic experimental observations made in [3], including the observation that the velocity of a Wigner crystal experiences saturation with increasing driving field.

The Bragg-Cherenkov scattering is *coherent many-electron* emission or absorption of vibrational excitations (surface phonons or ripplons). Conventional single-electron Cherenkov emission arises if the electron velocity $\mathbf{v}$ exceeds the phase velocity of irradiated waves $v_{\mathrm{ph}}(q)$, and the transferred momentum $\hbar\mathbf{q}$ is small compared to the electron momentum, in which case the energy conservation law is of the form $\mathbf{q} \cdot \mathbf{v} = \omega(q)$ [$\omega(q) \equiv q v_{\mathrm{ph}}(q)$ is the radiation frequency]. If the electrons form a solid, the Cherenkov waves emitted by different electrons interfere with each other. As in Bragg scattering, this interference is constructive for wave vectors of the irradiated waves equal to the reciprocal lattice vectors of the electron solid $\mathbf{G}$. The Bragg-Cherenkov scattering is just the result of this interference. It gives rise to a strong increase in the emission rate when the velocity of the electron solid is such that $\mathbf{v} \cdot \mathbf{G}/G$ becomes close to the phase velocity $v_{\mathrm{ph}}(G)$. Respectively, the reaction or frictional force $\mathbf{F}(\mathbf{v})$ should also dramatically increase for such velocities.

For finite temperatures, 2D solids do not have translational long-range order [5]. The density correlator decays as a power law of interparticle distance, for large distances [6]. This gives rise to smearing of the Bragg peaks, and in the case of Bragg-Cherenkov scattering should give rise to smearing of the peaks in the frictional force as a function of the velocity of electron solid. In particular, $\mathbf{F}(\mathbf{v})$ should have *tails* on the low-velocity sides of the Bragg-Cherenkov resonances at $\mathbf{G} \cdot \mathbf{v} = \omega(G)$. We show below that these tails play an important role in the nonlinear conductivity of a Wigner crystal.

In evaluating the frictional force $\mathbf{F}$ we will assume that the electron system is moving as a whole with a velocity $\mathbf{v}$, but other than that the electrons and surface vibrations are close to thermal equilibrium. This approximation is reasonable for comparatively small velocities where heating of the electron system is small, and for weak enough coupling to the vibrations. The coupling Hamiltonian is of the form

$$H_i = \sum_{\mathbf{q}} V_{\mathbf{q}} \rho_{\mathbf{q}} (b_{\mathbf{q}} + b_{-\mathbf{q}}^{+}), \qquad \rho_{\mathbf{q}} = \sum_n e^{i\mathbf{q}\cdot\mathbf{r}_n}, \qquad (1)$$

where $b_{\mathbf{q}}^{+}, b_{\mathbf{q}}$ are ripplon (or surface phonon) creation and annihilation operators ($\mathbf{q}$ is a 2D vector), and $\rho_{\mathbf{q}}$ is the electron density operator.

The average force per electron is given by the time derivative of the total electron momentum $\mathbf{P}$, $\mathbf{F} = -i(\hbar n S)^{-1}\langle[\mathbf{P}, H_i]\rangle$, where n is the electron density and S is the area of the system. To the lowest order in H_i, in the spirit of the memory function formalism [7] the electric current and the force are expressed in terms of the electron density correlator $\langle \rho_{\mathbf{q}}(t)\rho_{-\mathbf{q}}(0)\rangle_0$ for the isolated electron system [8,9]:

$$\mathbf{F}(\mathbf{v}) = -(\hbar n S)^{-1} \sum_{\mathbf{q}} \mathbf{q} \frac{\bar{n}(\omega(q)) + 1}{\bar{n}(\mathbf{q}\cdot\mathbf{v}) + 1} |V_{\mathbf{q}}|^2 \times \int_{-\infty}^{\infty} dt\, e^{i[\mathbf{q}\cdot\mathbf{v} - \omega(q)]t} \langle \rho_{\mathbf{q}}(t)\rho_{-\mathbf{q}}(0)\rangle_0 . \qquad (2)$$

Here, $\bar{n}(\omega) = [\exp(\hbar\omega/kT) - 1]^{-1}$ is the Planck number.

For electrons that form a Wigner crystal, the correlator $\langle \rho_{\mathbf{q}}(t)\rho_{-\mathbf{q}}(0)\rangle_0$ as a function of the wave vector $\mathbf{q}$ has sharp peaks at the reciprocal lattice vectors $\mathbf{G}$. For zero temperature and $S \to \infty$, these peaks are given by

$\delta(\mathbf{q} - \mathbf{G})$. It then follows from Eq. (2) that the zero-temperature force $\mathbf{F}_{T=0}$ is of the form

$$\mathbf{F}_{T=0} = -\frac{2\pi}{\hbar} nS \sum_{\mathbf{G}} \mathbf{G} |\tilde{V}_{\mathbf{G}}|^2 \delta[\mathbf{G} \cdot \mathbf{v} - \omega(G)], \qquad \tilde{V}_{\mathbf{q}} \equiv V_{\mathbf{q}} \exp(-\lambda^2 q^2/4), \tag{3}$$

where λ^2 is the mean square electron displacement from the lattice site for zero temperature [see Eq. (8) below].

The force (3) describes friction due to the Bragg-Cherenkov scattering, where surface waves with the Bragg wave vectors $\mathbf{G}$ are coherently emitted by all electrons. Clearly, $\mathbf{F}_{T=0}$ goes to infinity for resonant values of the velocity $\mathbf{v}$ defined by the condition $\mathbf{G} \cdot \mathbf{v} = \omega(G)$. We note that in the case of coupling to 3D vibrations one should perform integration in (3) over their transverse wave vector, and the δ functions will go over into the step functions. The occurrence of the related step functions in the absorption coefficient of a Wigner crystal at rest was shown in [10].

In (3) we have neglected the contribution from combined Bragg-Cherenkov processes where phonons of the Wigner crystal are emitted along with surface excitations. This contribution gives rise to smooth sidebands on the high-v sides of the peaks (3). It is small for "soft" surface excitations, such that

$$c_t n^{1/2} \gg \omega(G), \qquad c_t \gg d\omega(G)/dG, \tag{4}$$

where c_t is the transverse sound velocity of the Wigner crystal. For typical experimental parameters for electrons on helium $c_t n^{1/2}/\omega(G) \gtrsim 10^2$, for actual $G \leq \lambda^{-1}$.

In the case of finite temperatures the Bragg peaks in the static density correlator of the electron solid are smeared, $\langle \rho_{\mathbf{q}} \rho_{-\mathbf{q}} \rangle_0 \propto \sum_{\mathbf{G}} |\mathbf{q} - \mathbf{G}|^{-2+\alpha(G)}$ [6], where the temperature-dependent term in the exponent

$$\alpha(G) = \frac{kTG^2}{4\pi m c_t^2 n}. \tag{5}$$

To describe the related smearing of the δ-shape spikes (3) in the frictional force one should analyze the behavior of the *time-dependent* electron density correlator which is given, for a long time $t \sim |\mathbf{G} \cdot \mathbf{v} - \omega(G)|^{-1}$, by the asymptotic expression

$$\langle \rho_{\mathbf{q}}(t) \rho_{-\mathbf{q}}(0) \rangle_0 = nS \sum_n \exp[i\mathbf{q} \cdot \mathbf{R}_n - q^2 W(\mathbf{R}_n, t)], \qquad W(\mathbf{R}, t) \approx \frac{kT}{4\pi m c_t^2 n} \ln[\omega_m (t^2 + \kappa c_t^{-2} R^2)^{1/2}] + \frac{1}{2}\lambda^2, \tag{6}$$

Here, the vectors $\mathbf{R}_n$ specify the lattice sites, and $\omega_m = \min(\Omega, kT/\hbar)$ where Ω is the Debye frequency of the Wigner crystal; the coefficient κ is ~ 1. In (6) we dropped temperature-dependent terms in $W(\mathbf{R}, t)$ that are not logarithmically large for large $R^2 + c_t^2 t^2$.

The major contribution to the integral over $\mathbf{q}$ in Eq. (2) comes from the values of $\mathbf{q}$ close to the reciprocal lattice vectors $\mathbf{G}$. For slow surface waves (4) one can replace $\mathbf{q}$ by $\mathbf{G}$ everywhere except the fast oscillating factor $\exp(i\mathbf{q} \cdot \mathbf{R}_n)$ in the electron density correlator (6). It is straightforward then to integrate over $\mathbf{q} \approx \mathbf{G}$ for each $\mathbf{G}$, and then to evaluate the sum over R_n (cf. [11] where there were considered tails of the absorption lines due to coupled plasmon-ripplon resonances [12]). After evaluating the integral over time in (2) we obtain

$$\mathbf{F} = -\frac{nS}{\hbar\omega_m} \sum_{\mathbf{G}} \mathbf{G} \frac{\mathbf{G} \cdot \mathbf{v}}{\omega(G)} |\tilde{V}_{\mathbf{G}}|^2 \zeta(G) \times \left| \frac{\omega_m}{\mathbf{G} \cdot \mathbf{v} - \omega(G)} \right|^{1-\alpha(G)}, \qquad \zeta(G) = 2\sin[\pi\alpha(G)/2]\Gamma[1 - \alpha(G)], \tag{7}$$

where $\alpha(G)$ is given by Eq. (5), and we have set $kT \gg \hbar\omega(G), \hbar|\mathbf{G} \cdot \mathbf{v}|$ [the coefficient κ in (6) drops out of the expression (7) for slow surface waves (4)].

Equation (7) describes the tails of Bragg-Cherenkov resonances in the frictional force. These tails are formed as a result of multiphonon umklapp scattering processes where several thermal phonons of the Wigner crystal are created and annihilated, with the total change of the phonon energy equal to $\hbar|\omega(G) - \mathbf{G} \cdot \mathbf{v}| \ll kT$ and the total momentum transfer equal to G.

The frictional force (7) increases as a power law of the reciprocal detuning $|\mathbf{G} \cdot \mathbf{v} - \omega(G)|^{-1}$, with a fractional temperature-dependent exponent $1 - \alpha(G)$. This means that, in contrast to the situation for $T = 0$, there arises a strong frictional force even *before* the crystal reaches the critical velocity $v_{\mathrm{ph}}(G) = \omega(G)/G$ (for $\mathbf{v}$ parallel to $\mathbf{G}$). We note that in a nonlinear regime, where the $\mathbf{v}$-dependent terms in the denominators in (7) are substantial, the frictional force is not parallel to the velocity, except in the case where the crystal moves along a symmetry axis. In the general case, the crystal moves at an angle with respect to the driving force (which is equal to $-\mathbf{F}$ in stationary conditions). Equation (7) makes it possible to find the velocity for a given driving force. Clearly, this problem may have several solutions, and the velocity as a function of the driving force may display hysteresis.

For small velocities $|\mathbf{G} \cdot \mathbf{v}| \ll \omega(G)$, Eq. (2) provides a solution of the problem of the conductivity $\sigma = e^2 nv/F$ of a Wigner crystal weakly coupled to surface vibrations. This solution applies for temperatures small compared to the Debye temperature $kT \ll \hbar\Omega$. For such temperatures, the characteristic wave numbers of the surface vibrations involved in scattering are limited by the condition $q \lesssim \lambda^{-1}$, and $\alpha(q) \ll 1$ for such q (the conditions $\alpha(\lambda^{-1}) \ll 1$ and $kT \ll \hbar\Omega$ are equivalent). Comparison of the theory with the experimental results on the conductivity of an unpinned Wigner crystal [13] will be discussed elsewhere.

We note that Eqs. (6) and (7) apply also in the presence of a magnetic field normal to the electron layer. Magnetic field affects only the amplitude of zero-point vibrations λ

in (3) and the characteristic frequency Ω in (6), which in the strong field becomes the limiting frequency of the lower phonon branch of the Wigner crystal [14]:

$$\Omega = \frac{\omega_p^2}{(\omega_p^2 + \omega_c^2)^{1/2}}, \qquad \lambda^2 \sim \frac{\hbar}{m(\omega_p^2 + \omega_c^2)^{1/2}}, \qquad (8)$$
$$\omega_p = (2\pi e^2 n^{3/2}/m)^{1/2} \qquad (c_t \approx 0.2\omega_p n^{-1/2}),$$

where ω_c is the cyclotron frequency. In classically strong magnetic fields the nondiagonal component of the conductivity exceeds the diagonal one, $|\sigma_{xy}| \gg \sigma_{xx}$, and the velocity of the crystal $\mathbf{v} \approx \mathbf{v}_H$, where $v_H = cE/B$ is the Hall velocity in the crossed electric and magnetic fields **E** and **B**. In this case the dissipative conductivity σ_{xx}

$$\sigma_{xx} = \frac{nc^2}{B^2 v_H^2} \mathbf{v}_H \cdot \mathbf{F}(\mathbf{v}_H). \qquad (9)$$

Equations (7)–(9) make it possible to analyze the strongly nonlinear magnetoconductivity observed in [2,3] for electrons on liquid helium in classically strong magnetic fields. For actual wave numbers, the dispersion law of capillary waves on helium surface, ripplons, is superlinear, $\omega(q) \propto q^{3/2}$. Therefore, as the velocity v of the electron crystal is increasing, the resonant condition $\mathbf{G} \cdot \mathbf{v} = \omega(G)$ is first met for the minimal reciprocal lattice vector $G_1 = (8\pi^2 n/\sqrt{3})^{1/2}$. Respectively, if the Hall velocity $\mathbf{v}_H$ is pointing along $\mathbf{G}_1$, it should saturate as a function of the driving field E at the value $\omega(G_1)/G_1$. Such saturation was indeed observed in [3].

The results for the Hall velocity v_H as given by Eqs. (7) and (9) are compared in Fig. 1 with the experimental data [3]. We have used the expressions for the matrix elements of the electron-ripplon coupling $V_{\mathbf{q}}$ given in [15]. In Fig. 1 the velocity v_H is plotted vs the longitudinal (along the field **E**) component of the electron velocity, $v_l = \sigma_{xx}E/ne$. When solving Eq. (7) the force $\mathbf{F}(\mathbf{v})$ was averaged over orientations of **v** with respect to the crystal axes. This was done having in mind the Corbino geometry used in the experiment [3]. In this geometry, the electric field is applied in the radial direction, and it causes rotation of the electron crystal in the magnetic field. For different azimuthal angles, the velocity **v** is pointing in different directions. The current measured in [2,3] was related to the azimuthally-averaged radial velocity v_l.

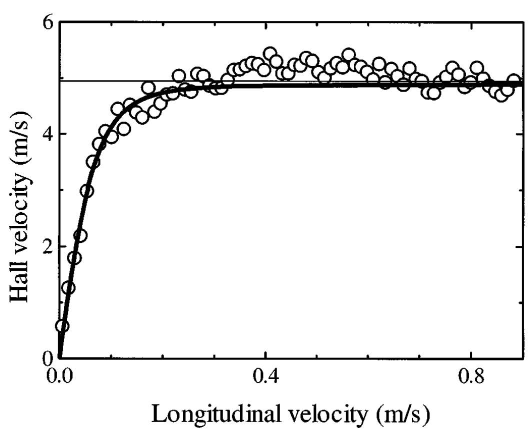

FIG. 1. The Hall velocity of an electron crystal on the helium surface vs the longitudinal velocity $v_l = \sigma_{xx}E/ne$. The bold line is the theory, the circles are the experimental data [3] for $n = 2.26 \times 10^8$ cm^{-2}, $T = 0.06$ K, $B = 0.2$ T. The thin line shows the ripplon phase velocity for the smallest reciprocal lattice vector of the crystal $v_{\mathrm{ph}}(G_1) = 4.95$ m/s.

Strong nonlinearity of the friction force substantially complicates the dynamics of a rotating electron crystal. In particular, the occurrence of the limiting velocity reminds the Ehrenfest paradox and, more generally, the problem of a rotating disc in the theory of relativity. In [3] the experimental data were analyzed in an assumption that the conductivity is spatially uniform, and the theoretical results in Fig. 1 refer to a uniformly moving Wigner crystal as well. Detailed analysis of the magnetoconductivity of a Wigner crystal in the Corbino geometry will be given elsewhere, including the effects of the shear deformation.

It is seen from Fig. 1 that, for small driving fields E, the Hall velocity v_H is proportional to v_l. The slope v_H/v_l for classically strong magnetic fields gives the value of the linear conductivity $\sigma_{xx} = (e^2 n/m\omega_c)v_l/v_H$, which is in good agreement with the experiment, without adjustable parameters. We note that the averaging over the directions of **v** we performed does not affect linear conductivity. Generally, the frictional force for small v_H is formed by the scattering processes with the momentum transfer $\hbar G \lesssim \hbar/\lambda$. However, for electrons on helium the actual values of G are much smaller because typically $\hbar\omega(G) \ll kT$ [4(b)], and the sum over **G** in (7) converges very fast and is not sensitive to the actual value of λ (in calculations we used the rhs of the expression (8) for λ).

With the increasing longitudinal velocity v_l, the Hall velocity v_H saturates at the value $v_{\mathrm{ph}}(G_1) = \omega(G_1)/G_1$. This is a consequence of the averaging over the directions of **v** in the Corbino geometry. The major contribution to the conductivity at saturation comes from the areas where **v** is nearly parallel to one of the six vectors $\mathbf{G}_1$. For saturated v_H, the conductivity is equal to $\sigma_{xx} = (e^2 n/m\omega_c)v_l/v_{\mathrm{ph}}(G_1)$, as first obtained empirically in [3], and is *proportional* to the current density nev_l. We note that the perturbation theory used to derive Eq. (7) does not apply deep in the range of saturation where $|\mathbf{G} \cdot \mathbf{v} - \omega(G)|$ is small and renormalization of coupled phonon-ripplon modes [12(b)] becomes substantial. The analysis of renormalization and decay of the coupled modes is necessary to describe the eventual switching of the system [1–3] to a low-conductivity state where $v_H \gg v_{\mathrm{ph}}(G_1)$ [3].

In conclusion, we have suggested a mechanism of many-electron scattering which is inherent to electron crystals and is due to coherent emission of surface waves with the wave vectors close to the reciprocal lattice vectors of the electron crystal. This mechanism, the Bragg-Cherenkov scattering, gives rise to strong nonlinearity of the electron transport as recently observed in the experiments.

We are grateful to M. J. Lea for useful discussions, and for providing us with the experimental data prior to publication. We also acknowledge valuable discussions with A. J. Dahm and P. M. Platzman. Y. G. R. is grateful for warm hospitality of Royal Holloway and Bedford New College, University of London, and of Michigan State University; his work was partly supported by the Royal Society.

*Permanent address: Institute of Semiconductor Physics, pr. Nauki 45, Kiev, 252028, Ukraine.

[1] L. Wilen and R. Giannetta, Solid State Commun. **78**, 199 (1991).

[2] K. Shirahama and K. Kono, Phys. Rev. Lett. **74**, 781 (1995); K. Kono and K. Shirahama, Surf. Sci. **361–362**, 826 (1996); J. Low Temp. Phys. **104**, 237 (1996).

[3] A. Kristensen *et al.*, Phys. Rev. Lett. **77**, 1350, (1996); A. Blackburn *et al.*, Czech. J. Phys. **46**, S1, 3056 (1996); M. J. Lea *et al.* (to be published).

[4] (a) T. Ando, A. B. Fowler, and F. Stern, Rev. Mod. Phys. **54**, 437 (1982); (b) *2D Electron Systems on Helium and Other Substrates*, edited by E. Y. Andrei (Kluwer Academic, New York, 1996); (c) for an introductory review on electrons on helium, see A. J. Dahm and W. F. Vinen, Phys. Today **40**, No. 2, 43 (1987).

[5] N. D. Mermin and H. Wagner, Phys. Rev. Lett. **17**, 1133 (1966); N. D. Mermin, Phys. Rev. **176**, 250 (1968).

[6] B. Jancovici, Phys. Rev. Lett. **19**, 20 (1967); Y. Imry and L. Gunther, Phys. Rev. B **3**, 3939 (1971).

[7] W. Gotze and P. Wolfle, Phys. Rev. B **6**, 1226 (1972); A. Isihara, Solid State Phys. **42**, 271 (1989).

[8] M. I. Dykman and L. S. Khazan, JETP **50**, 747 (1979).

[9] Yu. M. Vil'k and Yu. P. Monarkha, Sov. J. Low Temp. Phys. **15**, 131 (1989).

[10] N. Tzoar and P. M. Platzman, Phys. Rev. B **28**, 4844 (1983).

[11] M. I. Dykman, Sov. J. Low Temp. Phys. **10**, 233 (1984).

[12] (a) C. C. Grimes and G. Adams, Phys. Rev. Lett. **42**, 795 (1979); (b) D. S. Fisher, B. I. Halperin, and P. M. Platzman, Phys. Rev. Lett. **42**, 798 (1979).

[13] M. A. Stan and A. J. Dahm, Phys. Rev. B **40**, 8995 (1989); M. J. Lea *et al.* (to be published).

[14] H. Fukuyama, Solid State Commun. **19**, 551 (1976); L. Bonsall and A. A. Maradudin, Phys. Rev. B **15**, 1959 (1977).

[15] M. Saitoh, J. Phys. Soc. Jpn. **42**, 201 (1977).